Electric Motor Considerations for Non-Cryogenic Hybrid Electric and Turboelectric Propulsion

Kirsten P. Duffy[1]
University of Toledo, Cleveland, Ohio, 44135

NASA Glenn Research Center is investigating hybrid electric and turboelectric propulsion concepts for future aircraft to reduce fuel burn, emissions, and noise. Systems studies show that the weight and efficiency of the electric system components need to be improved for this concept to be feasible. However, advances in motor component materials such as soft magnetic materials, hard magnetic materials, conductors, thermal insulation, and structural materials are expected in the coming years, and should improve motor performance. This study investigates several motor types for a one megawatt application, and projects the motor performance benefits of new component materials that might be available in the coming decades.

I. Introduction

NASA Glenn Research Center is investigating hybrid electric propulsion and turboelectric propulsion for future aircraft to reduce fuel burn and emissions, and to enable technologies that will reduce aircraft noise. A study conducted by Boeing titled Subsonic Ultra Green Aircraft Research[1] showed that the use of hybrid electric propulsion significantly improved fuel burn and emissions for a 154-passenger aircraft. However, the weight and efficiency of the electric system components must be improved before hybrid electric or turboelectric propulsion is feasible. At NASA Glenn Research Center, Brown[2] performed an analysis of room temperature hybrid electric propulsion for a 150-passenger aircraft. He concluded that a motor with a total power density (motor and casing) of 4.9 kW/kg (3 HP/lb) and 97% efficiency would lead to an approximate 10% increase in aircraft weight. Much of this weight increase is due to battery weight. Continuing this effort, Jansen[3] has estimated the combinations of total electrical system power density and efficiency required to break even in a cost-benefit analysis for turboelectric aircraft, and is working on a similar analysis for hybrid electric propulsion.

To explore how non-cryogenic motors could be improved with better component materials and technologies, a study was performed by NASA Glenn Research Center's non-cryogenic hybrid electric propulsion team.[4] The final report predicted how component materials might improve within 15 and 30 years. Based on those conclusions, this study investigates several motor types for a one megawatt application, and projects the motor performance benefits of those new component materials.

Some motor types may be more advantageous for hybrid electric and turboelectric propulsion. Ganev[5] considered several electric machine types for use in high-performance power systems for applications such as more electric aircraft. The study ranked motors based on losses, thermal behavior, and power density, among other characteristics, with the conclusion that permanent magnet synchronous machines would be better suited than induction or switched reluctance machines.

For this study, permanent magnet, synchronous reluctance, and induction motors were selected for analysis. A baseline power level and fan size were chosen, and baseline motors were designed. Then the motor performance was predicted for the motors with current baseline materials (e.g. copper conductors, Hiperco laminations, NdFeB magnets), and then with the material properties that are projected for new advanced materials in the coming decades. In addition, a simple stress analysis was performed to highlight any structural concerns with a larger diameter tip drive motor.

A baseline application with a motor power level of 1 MW was chosen based on a small, eight-passenger aircraft. This motor size could also be used in a larger aircraft as part of a distributed propulsion system with multiple motor-driven fans. This motor size could also be more readily tested in the lab than the larger 10 MW motor that might be required for a 150-passenger aircraft, which is the ultimate goal. A target baseline was chosen of 96% efficiency and

[1] Senior Research Associate, NASA Glenn Research Center, 21000 Brookpark Road, MS 49-8, Cleveland, Ohio 44139, member AIAA.

5.8 kW/kg (3.5 HP/lb) based on electromagnetic weight alone (weight of rotor, stator, windings, and permanent magnets).

The fan speed of the aircraft was estimated to be 7000 RPM. A Numerical Propulsion System Simulation (NPSS) propulsor model was used to represent a free stream inlet module with a 1.3 pressure ratio fixed pitch (conventional) fan being driven by a 1 MW motor. The design point was an altitude of 30,000 feet and a Mach number of 0.8. The fan diameter was 0.80 m. It is assumed that the baseline motor drives the fan directly, although it is possible to use a gear box for this application. A gear box would add weight, but this could be offset by the lighter motor allowed by higher speed operation. The basic motor requirements are given in Table 1.

Parameter	Value
Power, P	1 MW
Speed, RPM	7000 RPM
Torque, T	1364 N-m
Target power density, PD	5.8 kW/kg (3.5 HP/lb)
Target minimum efficiency, η	96%
Fan diameter, D	0.80 m

Table 1. Baseline motor requirements

II. Assumptions

Several assumptions were made to guide the motor design. First, if the motor is directly driving the fan, it needs to be out of the airflow. Thus it was assumed that the motor would be either less than 0.5 m outer diameter ("standard" motor), or greater than 0.8 m inner diameter ("tip drive" motor). The motor diameter will have implications for the motor structural design. The larger the motor is for a given speed, the larger the stress will be within the motor rotor components. All the motors were designed with the rotor inside the stator.

The motor materials were assumed to be state-of-the-art. The windings consist of copper, the laminations are made of laminated Hiperco 50 which has high saturation flux density, and the magnets for the permanent magnet (PM) motors are made of neodymium iron boron (NdFeB) with a remanence flux B_r of 1.46. With the Hiperco 50, it was assumed that the flux density in the backiron would be set to 1.5 T and the stator teeth to 2.0 T. These are very high levels, chosen to reduce the mass of the laminations, increasing the power density. However, this high flux density also increases core loss.

The target electrical frequency was decided to be 1 kHz, which is fairly high. This frequency is set by the number of poles in the motor. The higher the number of poles, the smaller the backiron needs to be, again reducing weight and increasing power density. However, increasing the frequency will increase the core loss in the laminations, reducing efficiency.

The current density in the stator windings was assumed to be 10 A/mm^2, which is specified for "water or oil jacket" cooling, according to Gieras.[6] The number was assumed to be constant for all the motor performance analyses; however, adding better cooling would allow this number to increase, which could then affect the power density and efficiency. This is a parameter that can be investigated in future.

The motor assumptions are given in Table 2.

Parameter	Value
Standard motor outer diameter, OD	0.5 m maximum
Tip drive motor inner diameter, ID	0.8 m minimum
Stator winding current density, J	10 A/mm^2 rms maximum
Target flux density in stator and rotor teeth, B	2.0 T rms maximum
Target flux density in backiron, B	1.5 T rms maximum
Frequency, f	1 kHz
Baseline winding material	Copper
Baseline lamination material	Hiperco 50
Baseline permanent magnet material	NdFeB with B_r = 1.46 T

Table 2. Motor baseline design assumptions

III. Baseline and Projected Material Properties

The materials used in the motor performance analysis include winding material, lamination (soft magnetic) material, and PM (hard magnetic) material. The structural analysis includes the lamination material and PMs, as well as a carbon fiber epoxy composite wrap that contains the PMs for surface-mounted permanent magnet (SPM) motors.

Improvements to the winding material are expected as researchers find ways to incorporate the high electrical conductivity of carbon nanotubes (CNTs). Currently, wire made with CNTs has lower electrical conductivity than copper. However, improvements are expected in the future, and for the purposes of this study, a doubling of the electrical conductivity was assumed with the same winding material density.

For the lamination material, several properties are important. These include the flux density saturation level, the core loss as a function of frequency, and the tensile strength. The higher the saturation is the less lamination material is required in the motor, increasing the motor's power density. The core loss directly affects the efficiency of the motor. It can also affect the power density, since running the motor at a higher frequency allows for a smaller motor. Composite materials are currently being developed that incorporate hard and soft magnetic materials, improving the loss characteristics of the laminations but with lower saturation. For this study, it was assumed that the core loss would be reduced by 50% compared to the baseline Hiperco 50; however, the saturation level would be reduced to 75% of the baseline level.

Increasing the lamination tensile strength will allow the motor to run at a higher tip speed. This may enable the use of a tip drive motor in this application, with its blade tip speeds of Mach number 0.8. Higher lamination strength can also allow for higher speed standard motor design in general.

The PM material property varied in this study is the remanence flux, B_r. The air gap flux is proportional to B_r, and the torque is proportional to the air gap flux; therefore, increasing B_r increases the torque. It is expected that NdFeB PMs will have improved B_r of up to 1.75 T in the future.[4] Newer materials are currently being developed that incorporate hard and soft magnetic nanoparticles into a nanocomposite PM. These nanocomposites are expected to have a higher energy product than traditional PMs, and are expected to reach B_r of up to 2.0 T.[4] The analysis performed here includes PMs with B_r of 2.0 T.

Higher strength, lower weight structural materials will also benefit motor weight. Not only can these materials be used in the housing and motor mount, but also for containment of rotor parts, such as the PMs. A composite sleeve may be required for the SPM motor, which will occupy some of the air gap space, potentially resulting in a larger air gap. A stronger material enables a thinner sleeve to be used. Even if an inside-out motor design is used where the rotor is outside the stator, the lamination stress may be too high, also requiring a composite sleeve. In the structural analysis, it was assumed that the baseline carbon fiber epoxy material could be reinforced with CNTs, doubling the material strength.

NASA Glenn is also investigating insulation materials with high thermal conductivity, such those incorporating boron nitride nanotubes. These materials are expected to have a significant impact on motor performance through allowing a higher current density in the windings, and also allowing for a lower-weight cooling system. However, thermal analysis will be done in a separate study.

Table 3 shows the baseline and projected material properties used in this study.

Component	Baseline Material	Projected Material Property
Winding conductor	Copper	2 x electrical conductivity
Laminations	Hiperco 50	½ x loss with 75% B_{sat}
Permanent magnets	NdFeB with B_r = 1.46 T	B_r = 2.00 T
Composite sleeve	Carbon fiber epoxy	2 x strength

Table 3. Motor component material properties

IV. Baseline Motor Designs

Currently, the highest power density motors to date are PM motors; however, they are typically much smaller sized than the 1-MW required in this study (e.g. 5 kW for an axial flux PM motor which has a 5 HP/lb, or 8.2 kW/kg, continuous power density[7]). For this study, SPM motors, interior PM (IPM) motors, synchronous reluctance motors (SRMs), and induction motors (IMs) were investigated.

Originally, the power density had been identified as the key output variable. All of the motors were designed to maximize the power density. However, the efficiency is also a very important variable, especially for configurations where motor efficiency directly impacts the energy storage weight. It should be noted that any power density given here includes only the electromagnetic mass (rotor, stator, windings, and permanent magnets). It does not include the

shaft, bearings, cooling system, housing, or any other masses. The efficiency reported here only includes the resistive losses, core loss, and solid loss. The windage, bearing, or other losses were not calculated or assumed.

Many of the motor parameters are the same among the various designs. The air gap was chosen to be 1.5 mm, although this can depend on the number of poles. The magnet thickness was chosen to be 5 mm, which should give about 1 T magnetic flux in the air gap. The motor speed was set to 7000 RPM, although a gear box could be used to optimize the motor speed. Except for length, the stator dimensions were kept constant among all the standard motor designs, and the stator dimensions and rotor inner and outer diameter were kept constant among all the tip drive motor designs.

Motor design was performed using Motorsolve and RMxprt electromagnetic software packages. The final transient analyses were done using the Maxwell 2D electromagnetic finite element analysis software package. The analysis shows that not all of the baseline motors achieved the minimum power density and efficiency goals.

Of the standard motors, only the IPM motor met both targets. For the tip drive motors, the IPM and SRM motors met power density and efficiency goals. The best motor type for both standard and tip drive applications was the IPM motor. Note that the tip drive motors are significantly shorter than the standard drive motors. There may be benefits to one motor type versus the other in terms of incorporating the motors into the propulsion architecture.

Figures 1 and 2 illustrate the baseline standard and tip drive motors, and Table 4 details the dimensions, masses, and performance.

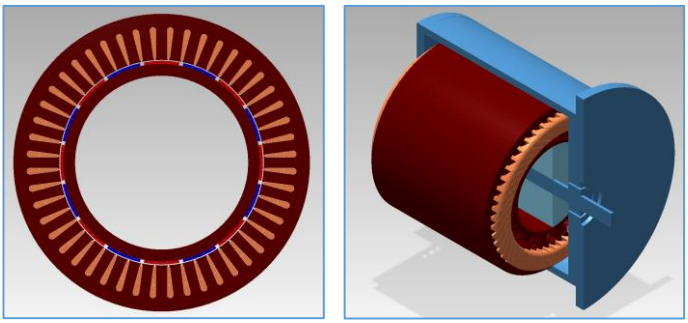

(a) SPM standard motor configuration

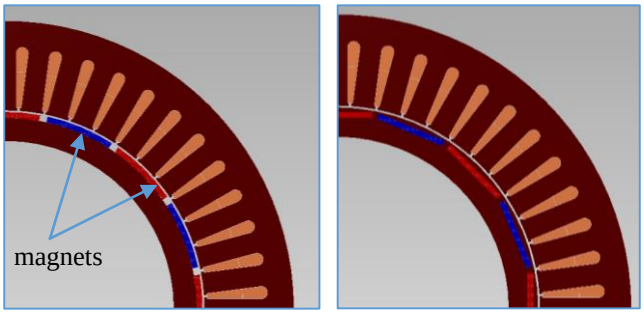

(b) SPM standard motor (c) IPM standard motor

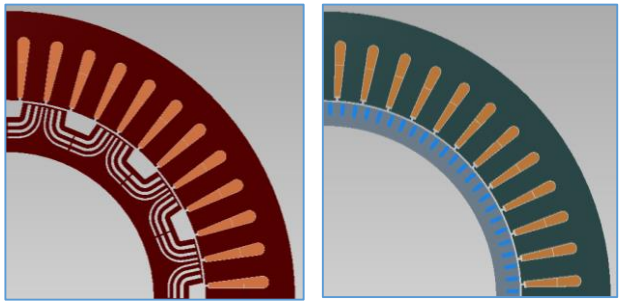

(c) SRM standard motor (d) IM standard motor

Figure 1. Baseline standard motor configurations

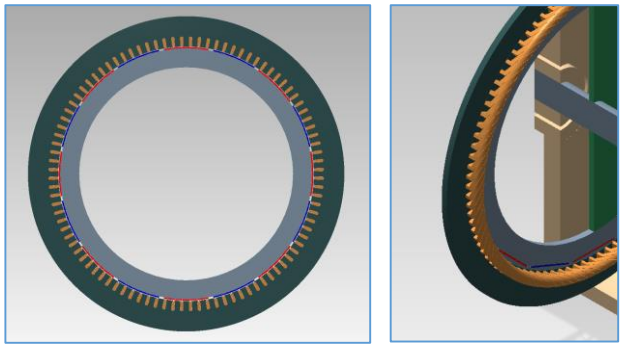

(a) SPM tip drive motor configuration

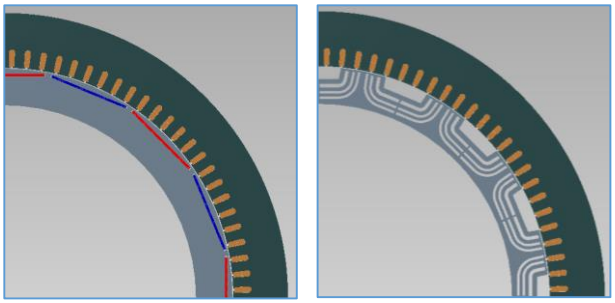

(c) IPM tip drive motor (d) SRM tip drive motor

Figure 2. Baseline tip drive motor configurations

	Standard Motor				Tip Drive Motor		
Parameter	**SPM**	**IPM**	**SRM**	**IM**	**SPM**	**IPM**	**SRM**
Outer diameter, OD (mm)	500	500	500	500	1184	1184	1184
Inner diameter, ID (mm)	292	292	255	290	800	800	800
Length, L (mm)	97	99	234	310	16.0	15.5	22.5
Stator copper mass (kg)	18.4	18.5	29.4	38.0	40.3	40.2	41.9
Stator core mass (kg)	58.3	59.5	140.7	186.8	39.3	38.1	55.3
Rotor copper mass (kg)	0.0	0.0	0.0	12.4	0.0	0.0	0.0
Permanent magnet mass (kg)	3.4	3.5	0.0	0.0	1.6	1.6	0.0
Rotor core mass (kg)	13.9	14.5	45.9	50.1	22.9	22.3	20.6
Total mass (kg)	94.0	96.1	216.0	287.2	104.1	102.2	117.7
Power density (kW/kg)	10.6	10.4	4.6	3.5	9.6	9.8	8.5
Efficiency (%)	95.3%	96.8%	93.7%	95.0%	91.6%	97.3%	96.8%

Table 4. Baseline standard motor types and performance for 16 poles at 1 MW

V. Motor Performance with Improved Material Properties

The motor performance in Table 4 includes only results with currently available materials. To see how these motors might perform with the improved materials, a study was made of the motors with changing conductor, lamination, and magnet materials. The idea was simply to change the materials in the baseline motor design and see the effect on power and efficiency. No motor design change was made based on the material changes. Obviously it would be best to optimize the motor design based on the material properties, and that will be done in the future.

Figure 3 shows the results of changing each motor component property individually. Figure 3a shows how the change in winding conductivity alone affects the winding loss. As expected, doubling the winding conductivity reduces the winding loss by half. However, for these particular motor designs, the losses are dominated by core loss and eddy current loss in the magnets. Therefore, reducing the winding loss has little effect on the motor efficiency. For a design with much higher winding loss, changing the conductor will be much more effective. Also, the tip drive motors have a higher percentage of windings in the end turns. This results in higher winding loss than the standard motors.

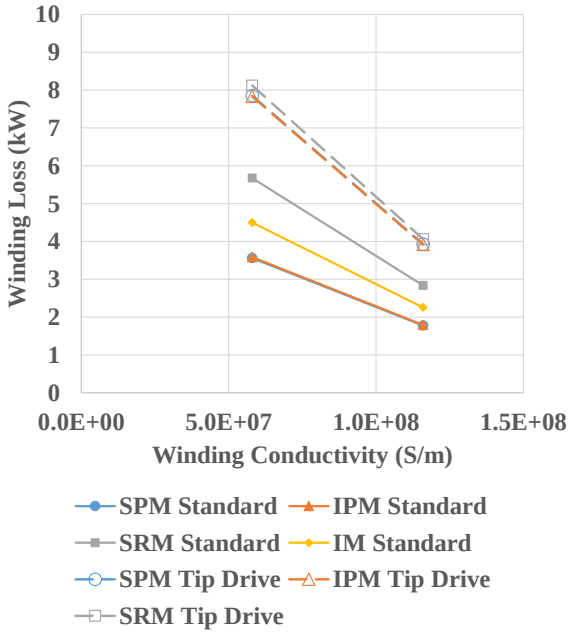

a. Winding loss vs. winding conductivity

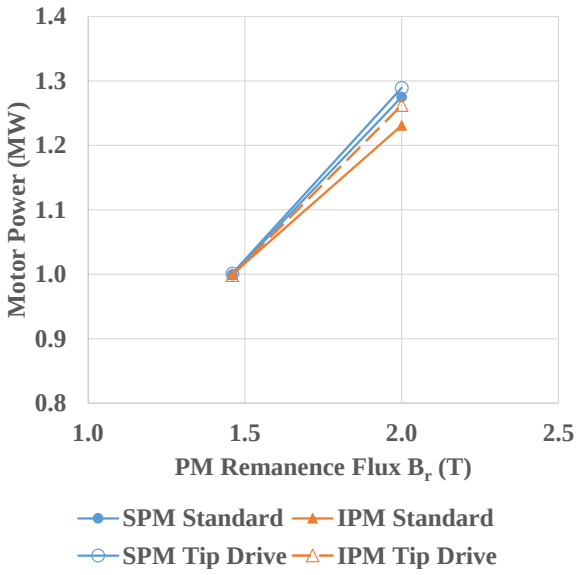

b. Motor power vs. PM remanence flux

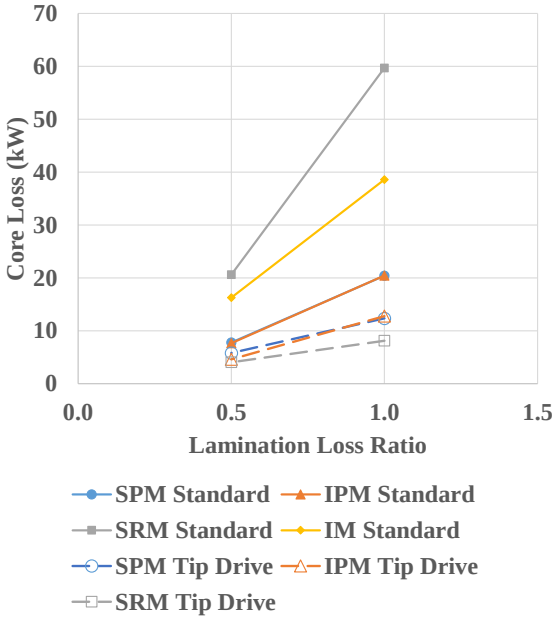

c. Core loss vs. ratio of lamination loss to baseline lamination loss

Figure 3. Effect of individual material changes on motor performance

Figure 3b shows how changing the magnet B_r alone increases the motor's power for the PM motors, while maintaining or improving efficiency. This can enable the motor to be shorter, increasing power density. Figure 3c shows how reducing the lamination loss, even while reducing the saturation flux, significantly reduces core losses. For these motor designs, the core loss is a dominating source of motor loss, and reducing core loss will have the biggest impact on motor efficiency.

An analysis was also done combining all the material improvements into each motor. First, the analysis was done with the improved material properties and the motor length adjusted to obtain 1 MW output power. Next, the analysis

was done with improved material properties, the winding current increased to give the same winding loss as the baseline motor, and the motor length adjusted to obtain 1 MW output power. Figures 4 and 5 show the results of this analysis compared to the baseline motor.

In the cases of the SRM and IM motors, the material improvements alone only serve to increase the motor efficiency, not the power density. In general, the losses from these motors were reduced by about 50%. However, reducing losses will also impact the weight of any cooling system, which should result in an improvement in total power density. When the winding current is increased again, then a power density benefit in the motor is achieved. The induction motor ended up with a 40% increase in power density, whereas the SRM standard and tip motors only increased power density by 6% and 10%, respectively.

The PM motors achieve a higher power density primarily due to the stronger magnets. For the standard SPM, increasing B_r from 1.46 to 2.00 alone increases the torque by 27%, allowing for a shorter motor to reach 1 MW. The improved materials alone allow for an approximate increase in power density of around 10%. Once the current is increased again to achieve the same baseline winding loss, the power density improves by about 35% for the standard PM motors and about 25% for the tip drive PM motors, compared to the baseline.

Of course, the lower conductor resistivity and lower core material loss increase the efficiency of the PM motors. The standard PM motors had a reduction of 50-55% in losses compared to the baseline with the improved materials alone, while the tip drive PM motors reduced losses by 37% for the SPM and 54% for the IPM. Once the current was increased to maintain the baseline winding loss, the loss was reduced by about 47% for the standard PM motors, 26% for the tip drive SPM motor, and 34% for the tip drive IPM motor, compared to the baseline.

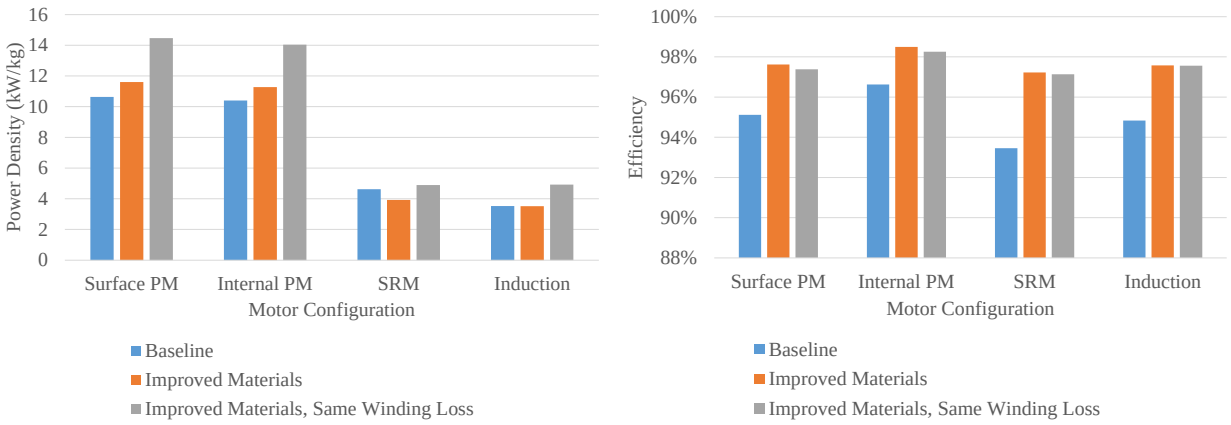

a. Power density (based on electromagnetic weight) b. Efficiency

Figure 4. 1-MW standard motor performance

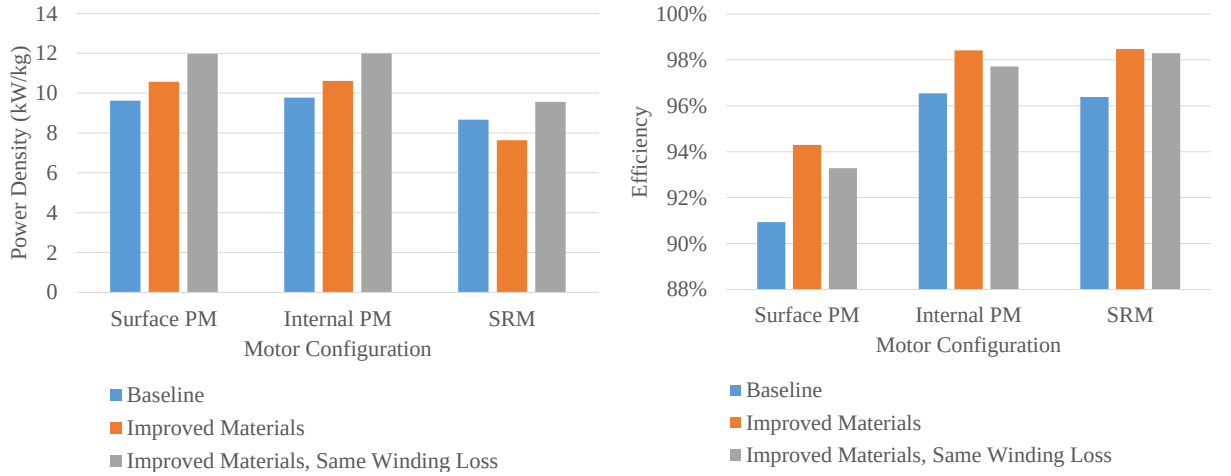

a. Power density (based on electromagnetic weight) b. Efficiency

Figure 5. 1-MW tip drive motor performance

It should be noted that for the SPM motor, there are significant eddy current losses within the PMs themselves. These losses are substantially reduced with an IPM configuration. Other ways of reducing these losses are through increasing the magnet thickness, decreasing the magnet circumferential length, or by segmenting the magnets. All of these actions also affect power density, so it is an iterative design process. Changing the material properties of the laminations and PMs did reduce the magnet loss by 22% for the standard SPM and 34% for the tip drive SPM, for the case with improved materials and baseline winding loss. The lamination loss change reduces the flux variation within the magnets, and the higher Br also results in a more consistent flux in the PMs.

VI. Structural Analysis

As the motor rotor spins, stresses result from centrifugal loading which are proportional to the square of the rotor tip speed. If we consider the tip drive motor, where the motor rotor is outboard of a fan with a tip speed of Mach 0.8, then the stresses can be extremely high. Arkkio[8] states that the maximum tip speed for a solid steel rotor is 400 m/s, for a high speed PM motor is 250 m/s, and for laminations is 200 m/s. The tip drive motors described here have tip speeds above 300 m/s.

The SPM designs will require a sleeve to contain the PMs. And if the laminations are segmented circumferentially to reduce lamination stress, there will need to be a sleeve to contain the rotor parts for the other motor types. This sleeve must be placed within the motor's air gap, potentially driving the air gap to be larger, impacting the motor performance. Even if an inside-out motor design were used, a sleeve would be required to contain the laminations in the tip drive rotor to keep the lamination stresses low. An analysis was done on the SPM motors to investigate the level of stress expected during operation.

Table 5 shows the strengths associated with the motor components.

Component	Material	Strength	Comments
Laminations	Hiperco 50	S_Y = 435 MPa S_{UT} = 814 MPa	Assume interference fit on ID
Magnets	NdFeB	S_{UT} = 80 MPa S_{UC} = 950 MPa	Assume no hoop stress since magnets are segmented
Composite sleeve	Toray T1000[9]	S_{UT} = 3040 MPa	Interference fit between sleeve and magnets

Table 5. Motor component material strengths

First, a simple analysis was performed to estimate the thickness of a composite sleeve required to contain the surface-mounted magnets alone. Here, we consider a simple composite ring of a given thickness, with a density that includes the weight of the magnets as well as the sleeve. Figure 6 shows the results for maximum sleeve hoop stress as a function of sleeve thickness at 7000 RPM. The graph shows that the sleeve thickness required to contain the magnets for the tip drive motor is approximately the size of the air gap thickness, before considering a factor of safety. Obviously the sleeve cannot fill the entire air gap, so the air gap would have to increase in size, degrading the performance of the motor.

It has been projected that the addition of carbon nanotubes (CNTs) to the carbon fiber composite could double the strength. While this might not be required for the standard SPM motor, it could enable the sleeve thickness to be reduced for the tip drive motor, allowing the air gap to remain small. For the tip drive example in Figure 7b, increasing the maximum stress from 3040 MPa to 6080 MPa reduces the sleeve thickness from 1.6 mm to less than 0.8 mm, again without considering a factor of safety or stress concentrations.

Next, an analysis of stresses within the laminations, magnets, and sleeve was performed for the SPM motor designs. This analysis ignores stress concentrations. The other rotor types will also have significant stresses (e.g. due to the complicated SRM rotor geometry with its thin flux paths, and magnet embedding for the IPM).

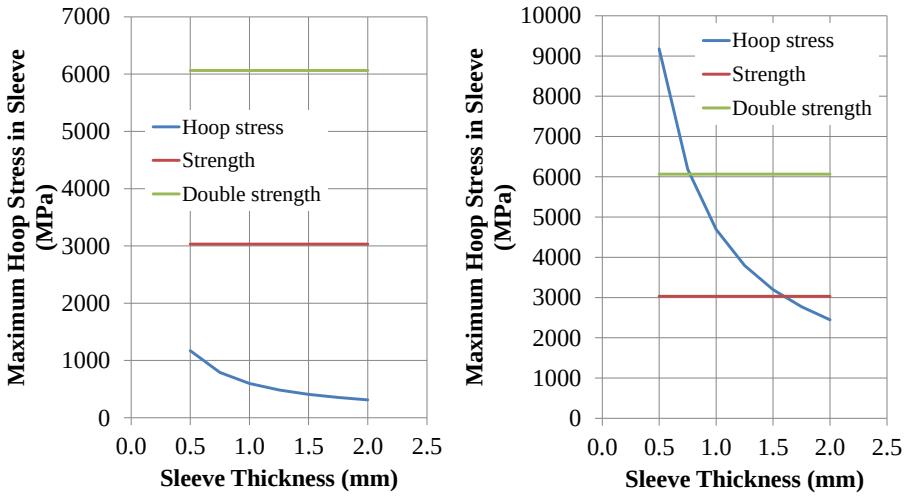

(a) Standard SPM rotor (b) Tip drive SPM rotor

Figure 6. Approximate sleeve hoop stress as a function of thickness at 7000 RPM

The closed-form equations for stresses and displacements for rotating cylinders in plane stress (thin disk) and plane strain (thick disk) can be found in Saada.[10] These equations were solved using Mathematica software to determine the stresses and displacements within the SPM motor components. The analysis assumes that the shaft, laminations, and composite sleeve are isotropic, and the segmented magnets are orthotropic. A carbon fiber composite sleeve is actually orthotropic; however, since the sleeve is very thin, the results are nearly the same. Also, the laminations are assumed to be solid, which is a worst case example, maximizing the hoop stress in the laminations.

We assume that none of the components separate from one another at any speed, so their displacements are the same at the interfaces, and the radial stress is the same and in compression at the interfaces. Also, since the magnets are segmented, they cannot sustain tensile hoop stress. Change in temperature was not considered in this analysis.

Table 6 shows the results of the stress analysis. We see again for the tip drive the sleeve hoop stress is very high, but also the lamination hoop stress is higher than the material yield strength. Unless the lamination material strength can also be increased in the future, the laminations would need to be segmented, increasing the sleeve stress even more.

This analysis indicates that if a tip drive motor is beneficial for the propulsion architecture, developing a sleeve material with increased strength may be required.

Parameter	**Standard SPM Rotor**	**Tip Drive SPM Rotor**
Rotor speed	7000 RPM	7000 RPM
Rotor tip speed	129 m/s	349 m/s
Sleeve thickness	0.6 mm	1.5 mm
Interference between laminations and shaft, δ_{12}	0.15 mm	1.5 mm
Interference between sleeve and magnets, δ_{34}	0.25 mm	4.5 mm
Radial stress between laminations and shaft	-13 MPa	-8.0 MPa
Radial stress between magnets and laminations	-0.2 MPa	-0.8 MPa
Radial stress between sleeve and magnets	-3.7 MPa	-9.5 MPa
Maximum hoop stress in laminations	189 MPa	845 MPa
Maximum hoop stress in magnets	0 MPa	0 MPa
Maximum hoop stress in sleeve	1104 MPa	2930 MPa

Table 6. Stress analysis results

VII. Conclusion

Several different radial flux motor configurations were considered for the 1MW fan drive application. They included standard and tip drive versions of SPM, IPM, and SRM motors, as well as a standard IM motor. The baseline

designs used currently available materials, including copper windings, Hiperco 50 rotor and stator laminations, and NdFeB permanent magnets. Of the baseline motor designs, only the standard IPM and tip drive IPM and SRM designs met the design objectives of 5.8 kW/kg and 96% efficiency.

With the incorporation of the improved materials (conductor, laminations, and PM), all of the motor designs saw increased power density and efficiency. The largest benefit occurred in the PM machines, primarily due to the more powerful magnets with Br increased from 1.46 T to 2.00 T. For example, the SPM standard motor improved from 10.6 to 14.5 kW/kg and 95.1% to 97.4% efficiency. Still, only the standard SPM and IPM and the tip drive IPM and SRM motors met the design objectives even after using the improved component material properties.

The primary driver in the design of all the 1-MW motors was high power density. However, it may be that efficiency is a more important parameter, since it will drive the size of the energy source required on the aircraft. For example, a small change in efficiency can mean an enormous change in battery size. With this in mind, the motors could be redesigned to have better baseline efficiency with reasonable power density, and the analysis with motor component materials be performed again.

The structural analysis highlighted the problems with a tip drive design. Fans are already designed for high blade tip speed. Having a motor rotor with a diameter larger than the fan will yield very high stresses in the rotor. The composite sleeve surrounding the magnets may require a thickness similar to the air gap thickness, leading to a bigger air gap with lower motor performance. The laminations themselves may have stresses that are too high for current core materials. Material strength improvements in laminations and sleeve material may enable use of a tip drive motor outboard of the fan tips.

Acknowledgments

This work was sponsored by the NASA Advanced Air Transport Technology Project of the Advanced Air Vehicle Program. The author thanks James Felder at NASA Glenn Research Center for performing the NPSS analysis.

References

[1]Bradley, Marty K. and Droney, Christopher K., "Subsonic Ultra Green Aircraft Research: Phase I Final Report," NASA/CR-2011-216847, 2011.

[2]Brown, Gerald V., "Efficient Flight-Weight Electric Systems," *NASA Fundamental Aeronautics Program 2012 Technical Conference*, Cleveland, OH, 2012.

[3]Jansen, Ralph H., Brown, Gerald V., Felder, James L., and Duffy, Kirsten P., "Turboelectric Aircraft Drive Key Performance Parameters and Functional Requirements," *AIAA Propulsion and Energy Conference*, Orlando, FL, 2015 (submitted for publication).

[4]Dever, T. P. et al., "Assessment of Technologies for Noncryogenic Hybrid Electric Propulsion," NASA/TP-2015-216588, 2015.

[5]Ganev, Evgeni, "Selecting the Best Electric Machines for Electrical Power-Generation Systems," *IEEE Electrification Magazine*, Vol. 2, Issue 4, Dec. 2014, pp. 13-22.

[6]Gieras, J. F., *Advancements in Electric Machines*, Springer, New York, 2008, p. 102.

[7]Long, G., "High Efficiency, High Power Density Electric Motors," *CAFE Technology Library* [online library], URL: http://cafefoundation.org/v2/pdf_tech/MPG.engines/HE_HP_electric_motors_Long_20090929.pdf [cited 19 May 2015].

[8]Arkkio, A., Jokinen, T. and Lantto, E., "Induction and Permanent-Magnet Synchronous Machines for High-Speed Applications," *Proceedings of the Eighth International Conference on Electrical Machines and Systems (ICEMS)*, 2005, pp. 871-876.

[9]"Toray CA T1000G Data Sheet," Technical Data Sheet No. CFA-008, Toray Carbon Fibers America, Inc. [online data sheet], URL: http://www.toraycfa.com/pdfs/T1000GDataSheet.pdf [cited 16 June 2015].

[10]Saada, A. S., *Elasticity: Theory and Applications*, Robert E. Krieger Publishing Co., Malabar, FL, 1974. Reprinted with corrections 1987.